Jpn. J. Appl. Phys. Vol. 41 (2002) pp. 1369–1373
Part 1, No. 3A, March 2002

Measurements of Third-Order Dispersion Effects for Generation of High-Repetition-Rate, Sub-Three-Cycle Transform-Limited Pulses from a Glass Fiber

Shinki NAKAMURA*, Liming LI[1], Naoki KARASAWA†, Ryuji MORITA, Hidemi SHIGEKAWA[2] and Mikio YAMASHITA

Department of Applied Physics, Hokkaido University, and CREST, Japan Science and Technology Corporation (JST), Kita-13, Nishi-8, Kita-ku, Sapporo 060-8628, Japan
[1]*Department of Photonics Material Science, Chitose Institute of Science and Technology, and CREST, Japan Science and Technology Corporation (JST), Chitose 066-8655, Japan*
[2]*Institute of Applied Physics and the Center for Tsukuba Advanced Research Alliance (TARA), University of Tsukuba, and CREST, Japan Science and Technology (JST), 1-1-1 Tennodai, Tsukuba 305-8573, Japan*

(Received July 30, 2001; accepted for publication November 27, 2001)

An active chirp compensator consisting of a prism pair and a spatial-phase-modulating pulse shaper enables us to accurately measure the third-order dispersion (TOD) dependence of the interferometric autocorrelation trace while keeping the optimum group-delay dispersion constant. As a result, it is shown that even a small change in TOD ($+60\,\mathrm{fs}^3$ and $-100\,\mathrm{fs}^3$) greatly affects the temporal pulse profile in the sub-8-fs region, and 92-fs pulses at a 75-MHz repetition rate from a laser-oscillator glass-fiber system is transform-limitedly compressed to 7.1 fs. [DOI: 10.1143/JJAP.41.1369]

KEYWORDS: active chirp compensation, few-optical-cycle pulse generation, spatial light modulator, glass-fiber nonlinear propagation, white light continuum

1. Introduction

Ultrashort pulse generation has advanced considerably in recent years, and optical pulses in the 4–5 fs regime have been generated by external pulse compression[1–4] with an amplifier at the repetition rate of 1 kHz and directly from Ti:sapphire lasers at the repetition rate of 100 MHz.[5,6] For chirp compensations, combinations of prism pairs, grating pairs and chirped mirrors have been employed.[1–6] However, such techniques have the disadvantages of interdependence among the group-delay dispersion (GDD), the third-order dispersion (TOD) and the higher-order dispersion, as well as bandwidth limitation and the inability to realize *in-situ* large phase adjustment without realignment. Therefore, accurate chirp compensation for the compression of few-optical-cycle pulses with ultrabroad spectra becomes increasingly difficult in the generation of shorter transform-limited pulses.

On the other hand, more recently, a novel pulse compression technique consisting of an Ar-gas-filled hollow fiber, a prism pair and a pulse shaper with a spatial light modulator (SLM) has been demonstrated for the generation of sub-5-fs amplified pulses at a repetition rate of 1 kHz.[7–9] This technique has the ability to overcome the above-mentioned problems. Using this technique, we clarify quantitatively and experimentally the relationship between the chirped pulse and the applied TOD under the obtained optimum GDD in the time region less than 10 fs, and demonstrate the generation of 7.1-fs transform-limited pulses which are output from a silica fiber (2.5 mm length) at a 75-MHz repetition rate. Single-mode silica optical fibers are attractive nonlinear media because of their low losses, small effective areas, low cost, commercial availability and the capability of broadband spectra generation by low energy pulses at a high repetition rate. To demonstrate accurate compensation, it is particularly important to use high-repetition-rate pulses because their stability is higher than that of an amplified pulse output from a hollow fiber at a low repetition rate. In addition, we will demonstrate that the SLM is an excellent device for controlling inter-independently the n-th order phase dispersion of chirped pulses even for the very small change in value of the n-th order dispersion. The use of nonamplified pulses, which have a stable intensity, enables us to demonstrate these issues for the first time.

To investigate the accurate chirp-compensation characteristics, we utilize a high-resolution, large SLM with 256 pixels,[10] whose one-pixel size is the same as previously reported but the total pixel number is doubled, and a frequency-resolved optical gating (FROG) apparatus to characterize the frequency-dependent phase of fiber output pulses before the chirp compensation experiment.

2. Experiment

Our experimental setup is shown in Fig. 1. The 12-fs, 10-nJ pulses with the center wavelength of 800 nm were generated from a mode-locked Ti:sapphire laser (Femtolaser GmbH, M-1) at the repetition rate of 75 MHz. The 12-fs

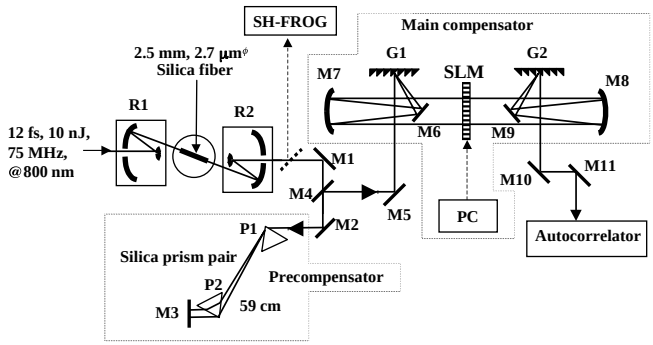

Fig. 1. Layout of the experimental setup. M1-6, M9-11, silver-coated plane mirrors; M7 and M8, silver-coated spherical mirrors, $R = -400$ mm; P1, P2, Brewster-angle cut silica prisms; G1,G2, gold-coated gratings $d = 300$ lines/mm; R1, R2, reflective objectives (36×); SLM, spatial light modulator controlled by computer (PC).

*Present address: Department of Media and Telecommunications Engineering, Ibaraki University, and CREST, Japan Science and Technology Corporation (JST), 4-12-1, Nakanarusawa, Hitachi, Ibaraki 316-8511, Japan. E-mail address: nakamura@dmt.ibaraki.ac.jp
†Present address: Department of Applied Photonics System Technology, Chitose Institute of Science and Technology, and CREST, Japan Science and Technology Corporation (JST), Chitose 066-8655, Japan.

pulses were coupled into a 2.5-mm silica fiber by a 36x reflective objective R1 (Ealing) which was made of gold mirrors and introduced no additional phase dispersion for the 12-fs pulses. The silica fiber was a polarization-preserving single-mode fused silica fiber (Newport, F-SP-V) with a core diameter of 2.7 μm. The coupling efficiency was measured to be 27%. The output from the 2.5-mm fiber was collimated by another objective R2 (Ealing) made of aluminum mirrors and its spectrum was measured by a spectrometer. In addition, the output pulse was characterized by our second-harmonic generation FROG (SHG-FROG) apparatus.

With an input pulse power of 120 kW, the fiber output spectrum was broadened due to the dispersive SPM effect, and the broad-spectral pulse had a duration of 92 fs. The chirped pulse was first precompensated by a pair of fused-silica Brewster prisms P1 and P2 with a separation length of 59 cm. The output pulse from the prism pair was coupled into a 4-f pulse-shaping apparatus[7–12] which consisted of a pair of 300 lines/mm gold-coated gratings G1 and G2 (Richardson Grating Laboratory) placed at the focal planes of a pair of 200-mm-focal-length concave-spherical silver mirrors M7 and M8. A programmable one-dimensional 256-pixel SLM (custom-made by BNS Inc.) with a total effective width of 27 mm and a height of 10 mm was set on the Fourier plane at the center of the two spherical mirrors between the two gold-coated gratings. In the SLM, each pixel had a width of 100 μm and an inter-pixel gap of 7 μm. This pulse-shaping apparatus was nondispersive except for the SLM. The total transmission efficiency of the SLM pulse-shaping system including the losses of many reflection components was about 20%. The chirp-compensated pulses from the pulse shaper were measured by an interferometric autocorrelator with a 25-μm-thick BBO crystal (Femtolaser GmbH). We were unable to employ the SHG-FROG technique for the measurement of the pulse shaper output because the power of the compensated pulse was below the sensitivity of our FROG apparatus.

The main-chirp compensation by the computer-controlled SLM in the 4-f configuration was carried out by a procedure similar to that previously reported.[7–9] The spectral phase to be applied by the SLM, $\phi(\omega_j)$, is described by the following equation:

$$\phi(\omega_j) = \frac{1}{2!} \times \phi'' \times (\omega_j - \omega_0)^2 + \frac{1}{3!} \times \phi^{(3)} \times (\omega_j - \omega_0)^3 + \cdots, \quad (1)$$

where $j = 1, 2, \ldots, 256$ (the pixel number), $\phi'' \equiv d^2\phi(\omega)/d\omega^2|_{\omega_0}$ and $\phi^{(3)} \equiv d^3\phi(\omega)/d\omega^3|_{\omega_0}$ at the center angular frequency $\omega_0 = \omega_{128}$ of the pulse spectrum (the corresponding wavelength $\lambda_0 = 800$ nm at the incidence angle $\theta_i = 0$) correspond to GDD and TOD, respectively, and $\omega_j - \omega_0$ represents the angular frequency difference between the jth pixel and the 128th pixel. The angular frequency ω_j is given by $\omega_j = 2\pi c/\lambda_j$, where c is the velocity of light in vacuum. The jth pixel wavelength λ_j is expressed with respect to the spatial position x_j as $\lambda_j = [d\{\sin(\tan^{-1}(x_j/f) + \sin(\lambda_c/d)) + \sin\theta_i\}]$.[7,9,13–16] $x_j = j\Delta x$, and Δx is the pixel width for the SLM. f denotes the focal length of the so-called 4-f configuration SLM compensator. The numerical result of our 4-f SLM chirp compensator is depicted by the upper and lower horizontal axes in Fig. 3.

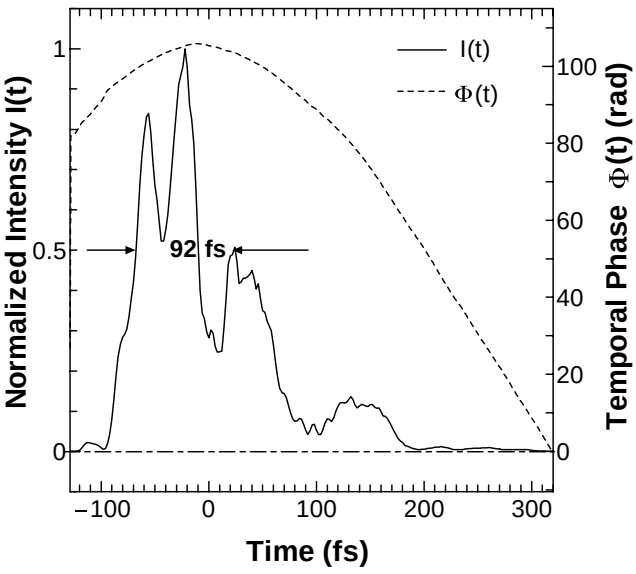

Fig. 2. The FROG-retrieved intensity profile, $I(t)$, and phase, $\Phi(t)$, of the pulse as a function of time for silica-fiber output.

3. Active Chirp Compensation

To find the optimum distance between two prisms for precompensation and the optimum spectral phase retardation to be applied by the SLM for main compensation, we measured the temporal intensity and phase profiles of the output pulses from the silica fiber using an SHG-FROG apparatus (25-μm-thick BBO). The pulse was retrieved well, with a FROG error of 0.012 for a 512 × 512 pixel trace. The number of delay points was 512 with the delay-time spacing of 2.0 fs, and the number of wavelength points was 512 with the wavelength spacing of 0.45 nm. Figure 2 shows the retrieved temporal intensity $I(t)$ and phase $\Phi(t)$ profiles of the pulse. The pulse width (full width half maximum, FWHM) of the temporal intensity profile with the large structures was 92 fs and the FWHM of the intensity autocorrelation was 135 fs. The change in temporal phase was nearly 100 radians and the chirp, $\delta\omega(t) = d\Phi(t)/dt$, indicated a relatively large nonlinearity as a function of time. When the retrieved spectral phase $\phi(\omega)$ was extrapolated at the center angular frequency ω_0 using an equation similar to eq. (1), the GDD and TOD values at $\lambda_0 = 800$ nm were determined to be $\phi'' = +342\,\text{fs}^2$ and $\phi^{(3)} = +187\,\text{fs}^3$, respectively.

In order to precompensate for the previously obtained large GDD, namely, the linear chirp part of fiber output pulses, the prism distance was set at 59 cm to impart a negative GDD value of $-342\,\text{fs}^2$ at 800 nm (calculation from ref. 17) with the TOD value of $-479\,\text{fs}^3$. Here, the linear chirp indicates that $d\Phi/dt$ is proportional to time t, and it is known that $d\Phi/dt \cong [1/\phi''(\omega_0)] \times t$ for the Gaussian pulse and $\phi^{(3)}(\omega_0)$ causes nonlinear chirp in the time domain. Similar calculations indicated that the GDD and TOD values at 800 nm for the fused-silica SLM substrates of a total thickness of 4.6 mm were $+165\,\text{fs}^2$ and $+125\,\text{fs}^3$, respectively, while dispersion of the 10-μm-thick liquid crystal was neglected.

Based on these considerations (see Table I), the GDD of

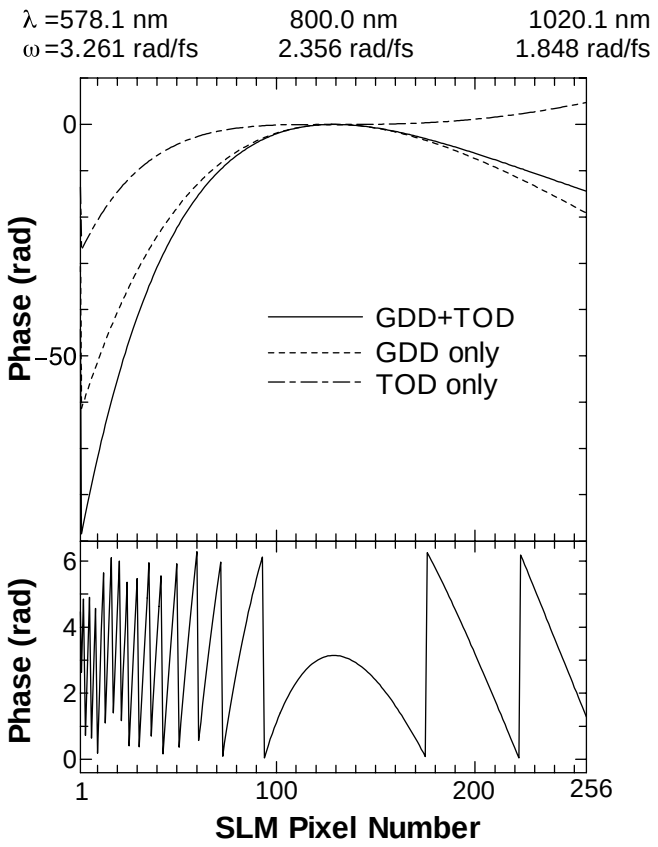

Fig. 3. Applied phase distribution as a function of the SLM pixel number and corresponding folded phase distribution.

Table I. Evaluated dispersion for 800 nm from FROG measurements and various optical components, and applied GDD and TOD.

Optical components	GDD (fs^2) at 800 nm	TOD (fs^3) at 800 nm
Silica fiber output	342	187
Silica prism pair (59 cm) (2.5 mm, 2.7 μm^{ϕ}, 12 fs, 120 kW)	−342	−479
SLM substrate (4.6 mm silica)	165	125
GDD, TOD applied by SLM	**−150**	**220**
Total	+15	+53

$-150\,fs^2$ and the TOD of $+220\,fs^3$ at 800 nm were applied by the SLM in the 4-f configuration for main-chirp compensation, as shown in Fig. 3, where the phase as a function of the pixel number was folded at each pixel exceeding $2\pi N$ radians ($N = 1, 2, 3 \ldots$) as in the previous reports.[11,18] Regarding the GDD value, the optimum result was not obtained when the GDD of $-165\,fs^2$ was applied. As shown at the top of Fig. 3, the largest angular frequency through the SLM was 3.261 rad/fs at the 1st pixel and the smallest angular frequency was 1.848 rad/fs at the 256th pixel, and the carrier angular frequency ω_0 was 2.356 rad/fs located at the 128th pixel. Corresponding wavelengths for the angular frequencies are also shown at the top of Fig. 3, and suggest that the use of diffraction gratings results in a spatial dispersion that is nearly proportional to the wavelength.

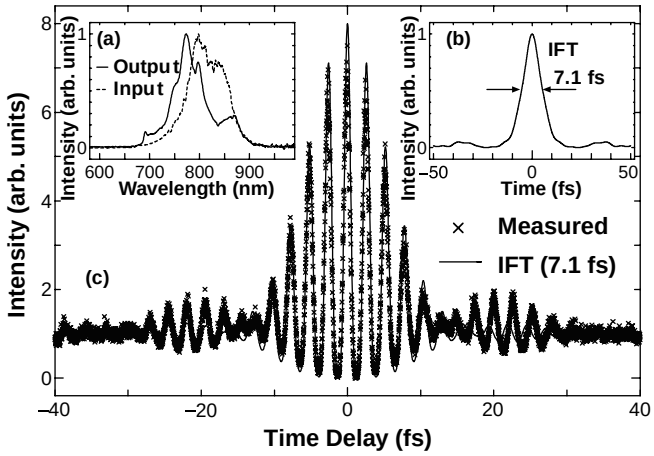

Fig. 4. (a) Measured pulse spectrum (solid line) from the 4-f pulse shaper under optimum GDD and TOD values of $-150\,fs^2$ and $+220\,fs^3$, respectively. The dashed line shows the measured input spectrum of the fiber. (b) Inverse Fourier transformation (IFT) of the solid line of Fig. 4(a) with 7.1 fs FWHM. (c) The corresponding measured interferometric autocorrelation trace (cross points). The solid line is a fit from the above IFT.

As a result of applying the phase shown in Fig. 3 to the SLM, the interferometric autocorrelation (IAC) trace as shown in Fig. 4 (cross points) was observed. The power of the compensated pulse was below the sensitivity of our FROG apparatus. We also calculated the IAC trace of the 7.1-fs transform-limited pulse (the solid line in Fig. 4) which was obtained from the measured spectrum ranging from 670 to 930 nm at the pulse shaper output [the solid line of inset (a) in Fig. 4]. The good agreement between the two IAC traces suggested that 7.1-fs transform-limited pulses were generated. The IAC calculated for small GDD and TOD values was rather deviated from the best fitting curve which was calculated from the inverse Fourier transform of the measured spectrum. To the best of our knowledge, these were the shortest pulses generated with the combination of a silica fiber and the SLM by non-amplified pulses. The small residual phase error shown in Table I might be due to the slight deviation from the dispersion-free distance of the grating pair forming the 4-f configuration.

It should be noted that this SLM technique for chirp compensation has two limitations. First, the difference of phases imparted on two neighbor-pixels in the SLM, $\Delta\phi = \phi_i(\omega_i) - \phi_{i+1}(\omega_{i+1})$, where $i = 1, 2, \ldots, 255$, should be less than π.[15,18] Second, the longest $t_{\mathrm{p.in.max}}$ to be compensated for should be much shorter than the time window $t_w = \lambda_0 D/c\, d \cos\theta_d$ ($\cong 2.0$ ps) of the 4-f configuration in order to satisfy the condition of the Fourier transformation in the SLM plane (along the x axis).[19,20] Here, D and θ_d represent the incident beam diameter to the first grating and the diffraction angle at the central wavelength of λ_0, respectively.

4. Third-Order Dispersion Effect

We investigated the TOD dependence of the IAC trace while keeping the GDD ($-150\,fs^2$) constant (Fig. 5). First, we measured the shortest IAC trace of Fig. 4 [and Fig. 5(d)] under the best chirp compensation by the SLM. This trace indicated the expected ratio of 8 : 1 : 0 (the ratio among the

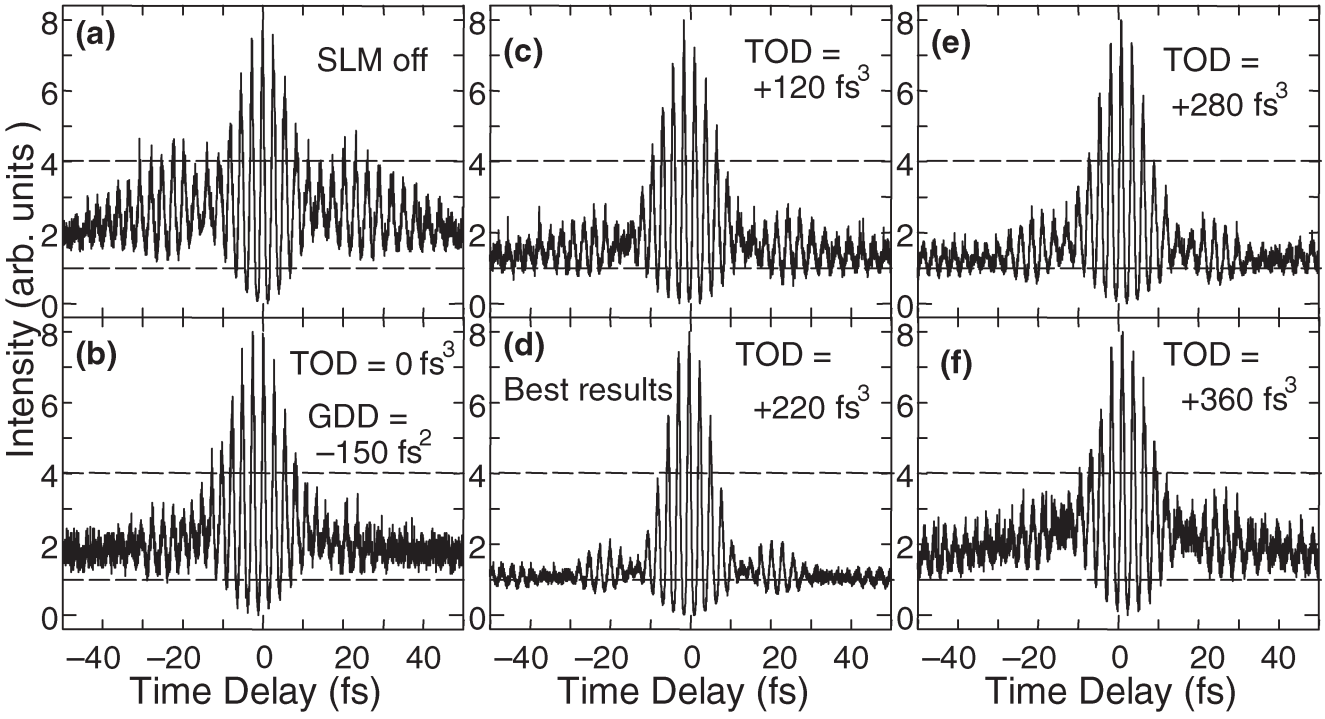

Fig. 5. Measured interferometric autocorrelation traces: (a) with no dispersion applied by the spatial light modulator; (b)–(f) as a function of different TOD values while keeping the GDD value constant at $-150\,\mathrm{fs}^2$.

absolute maximum, the background and the absolute minimum of the IAC trace), and agreed with the transform-limited pulse obtained from the measured spectrum. Therefore, we concluded that the alignment and the operation of our IAC apparatus were correct for this measurement. Next, we measured the remainder of the traces [Figs. 2(a) to 2(c) and 2(e) to 2(f)] without any realignment of our IAC apparatus by changing only the TOD values and keeping the GDD value [except for (a) where we were off the applied electric field of the SLM], using the computer-controlled SLM. This is one of the advantages of the SLM method, and implies that the measurements of (a) to (c) and (e) to (f) were also correct and these traces have the expected ratio of 8 : 1 : 0 for a long delay time.

When the applied GDD and TOD were both zero [Fig. 5(a)], the large substructure appeared in the IAC trace, where the background in the far time region from the peak was appropriately low. However, when only the GDD was set at $-150\,\mathrm{fs}^2$ [Fig. 5(b)], the relative amplitude of the off-center features decreased. With increasing only the TOD from $+120$ to $+220\,\mathrm{fs}^3$, a good peak-to-background ratio of 8 : 1 was observed and the small wing corresponding to the transform-limited pulse profile [the inset (b) in Fig. 4] appeared. A further increase of the TOD from $+280$ to $+360\,\mathrm{fs}^3$ again yielded off-center features which slightly differed from earlier observations. These results suggest that even a small change in TOD ($+60\,\mathrm{fs}^3$ and $-100\,\mathrm{fs}^3$) greatly affects the temporal intensity profile of the pulse in the 7-fs regime. The difference between the cases of the TOD increase and decrease may be due to the yielding of the relative difference between the GDD phase distribution and the TOD phase distribution in the high-frequency region (see Fig. 3), where the frequency width per pixel becomes larger and hence the phase difference between one pixel and its neighbor exceeds the critical value of π.[15,18]

5. Conclusions

We experimentally and quantitatively demonstrated that the change in the small value of the TOD of $+60\,\mathrm{fs}^3$ and $-100\,\mathrm{fs}^3$ at 800 nm was highly sensitive to the generation of 7.1-fs transform-limited pulses of sub-three optical cycles. The 92-fs pulses at a 75-MHz repetition rate from the short glass fiber were compressed for the first time to become 7.1-fs transform-limited pulses using a fused-silica prism pair and a 256-pixel-SLM pulse shaper that *in-situ* adjusts independently and accurately any order dispersions without physically realigning any optics. This extremely accurate and flexible SLM chirp compensator can be applied to the clarification of the compensation mechanism of the complicated phase when this method is combined with the adaptive feedback system.[11] It should be noted that this nonlinear chirp compensator with the ultrabroad bandwidth (from 480 nm to 1250 nm whose wavelength range is based on our previous experiments[7–9,14,16]) can be applied for complete chirp compensation of the one-octave-exceeding bandwidth pulse from the recently developed photonic crystal fibers[21] and tapered fibers.[22]

1) Z. Cheng, G. Tempea, T. Brabec, K. Ferencz, C. Spielman and F. Krausz: *Ultrafast Phenomena XI*: eds. T. Elsaesser, J. G. Fujimoto, D. A. Wiersma and W. Zinth (Springer-Verlag, Berlin, 1998) p. 8.
2) A. Baltuška, Z. Wei, M. Pshenichnikov and D. Wiersma: Opt. Lett. **22** (1997) 102.
3) M. Nisoli, S. D. Silverstri, O. Svelto, R. Szipöcs, Ch. Spielmann, S. Sartania and F. Krausz: Opt. Lett. **22** (1997) 522.
4) A. Shirakawa, I. Sakane, M. Takasaka and T. Kobayashi: Appl. Phys. Lett. **74** (1999) 2268.
5) U. Morgner, F. X. Kärtner, S. H. Cho, Y. Chen, H. A. Haus, J. G. Fujimoto, E. P. Ippen, V. Scheuer, G. Angelow and T. Tschudi: Opt.

Lett. **24** (1999) 411.
6) D. H. Sutter, G. Steinmeyer, L. Gallmann, N. Matuschek, F. Morier-Genoud and U. Keller: Opt. Lett. **24** (1999) 631.
7) L. Xu, L. Li, N. Nakagawa, R. Morita and M. Yamashita: IEEE Photonics Technol. Lett. **12** (2000) 1540.
8) L. Xu, N. Nakagawa, R. Morita, H. Shigekawa and M. Yamashita: IEEE J. Quantum Electron. **36** (2000) 893.
9) N. Karasawa, L. Li, A. Suguro, H. Shigekawa, R. Morita and M. Yamashita: J. Opt. Soc. Am. B **18** (2001) 1742.
10) S. Nakamura, L. Li, N. Karasawa, R. Morita, H. Shigekawa and M. Yamashita: *Twelfth Int. Conf. Ultrafast Phenomena XII, Charleston, South Carolina, July 12, 2000* (Optical Society of America, Washington D.C., 2000) OSA Technical Digest Series, WE4, p. 611.
11) D. Yelin, D. Meshulach and Y. Silberberg: Opt. Lett. **22** (1997) 1793.
12) A. M. Weiner: Rev. Sci. Instrum. **71** (2000) 1929.
13) A. Efimov, C. Schaffer and D. H. Reitze: J. Opt. Soc. Am. B **12** (1995) 1968.
14) M. Hirasawa, N. Nakagawa, M. Shibata, R. Morita, H. Shigekawa and M. Yamashita: *Conf. Laser and Electro-Optics, Baltimore, Maryland, May 6–11, 2001* (Optical Society of America, Washington D.C., 2001) OSA Technical Digest Series, CWA8, p. 270.
15) M. Yamashita, K. Matsumoto and L. Xu: Rev. Laser Eng. **28** (2000) 492 [in Japanese].
16) L. Li, S. Kusaka, N. Karasawa, R. Morita H. Shigekawa and M. Yamashita: Jpn. J. Appl. Phys. **40** (2001) L684.
17) R. L. Fork, C. H. Cruz, P. C. Becker and C. V. Shank: Opt. Lett. **12** (1987) 483.
18) A. Weiner, D. E. Leaird, J. S. Patel and J. R. Wullert, II: IEEE J. Quantum Electron. **28** (1992) 908.
19) F. Shimizu: Jpn. J. Appl. Phys. **26** (1987) L53.
20) N. Morita, R. Morita, N. Karasawa, H. Shigekawa and M. Yamashita: *Conf. Laser and Electro-Optics Pacific Rim, Chiba, Japan, July 15–19, 2001* (Optical Society of America, Washington D.C., 2001) OSA Technical Digest Series, WJ2-4.
21) J. K. Ranka, R. S. Windeler and A. J. Stentz: Opt. Lett. **25** (2000) 25.
22) T. A. Birks, W. J. Wadsworth and P. St. J. Russell: Opt. Lett. **25** (2000) 1415.